



INTERACTION OF LOCAL SUPERSONIC REGIONS ON A PROJECTILE MODEL

Alexander Kuzmin and Konstantin Babarykin

Department of Fluid Dynamics, St. Petersburg State University, Russia

E-Mail: a.kuzmin@spbu.ru

ABSTRACT

The 3D turbulent flow over a boat-tailed projectile is studied numerically at free-stream Mach numbers from 0.932 to 0.965 and the angle of attack of 6 deg. Formation and interaction of shock waves and local supersonic regions is scrutinized. Solutions of the Reynolds-averaged Navier-Stokes equations are obtained on unstructured meshes with finite-volume solvers of second-order accuracy. The solutions demonstrate intricate behavior of the pitching moment coefficient as a function of the free-stream Mach number. This is accounted for by interplay of local supersonic regions on the upper and lower surfaces of the projectile.

Keywords: transonic flow, local supersonic regions, shock waves, interaction.

1. INTRODUCTION

There are a number of works addressing transonic flow over non-spinning and spinning projectiles. In 1980s, it was established in wind-tunnel and ballistic measurements that aerodynamic characteristics of boat-tailed projectiles change intricately at high subsonic speeds of flight. With increasing free-stream Mach number M_∞ at a positive angle of attack α , the normal aerodynamic force drops rapidly to a so-called "critical point" before rising sharply to another critical point from which it drops once again. Sahu & Nietubic [1] carried out numerical simulations of 3D turbulent flow over several projectiles in a range of free-stream conditions using a $k-\varepsilon$ and algebraic eddy viscosity turbulence models. The calculated pitching moment and normal force were in good agreement with experimental data documented in free flights.

Budge [2] performed computations of 3D flow past ogive-cylinder projectiles using the OVERFLOW solver and a Baldwin-Barth turbulence model. He studied flow evolution with increasing M_∞ at $\alpha=4$ deg and confirmed the "transonic critical behavior" of the pitching moment and normal force. Shock wave locations were shown to influence the pressure distribution over the projectile and cause a decrease in the normal force before the first critical point, $M_\infty = 0.91$. The loss in normal force after the second critical point, $M_\infty = 0.97$, was interpreted as a consequence of the shorter recovery distance between the shock terminating the leading supersonic region and the boat-tail shock. Both critical points corresponded to flow fields with two separate supersonic zones on the projectile.

Lun [3] investigated the aerodynamic properties of a standard M549, 155 mm projectile. The research was focused on the transonic speed range. Aerodynamic data from wind tunnel testing was benchmarked against aerodynamic prediction programs ANSYS CFX and Aero-Prediction 09 (AP09). Next, a comparison was made between two types of angle of attack generation methods in ANSYS CFX. The research also focused on controlled tilting of the projectile's nose to investigate the resulting

aerodynamic effects. ANSYS CFX was found to provide better agreement with the experimental data than AP09.

In the 1990s and 2000s, numerical simulations of transonic flow over airfoils revealed instability of double supersonic regions on airfoils comprising a flat or nearly flat arc [4-6]. The instability is caused by an interaction between the shock wave, which terminates the bow supersonic region, and the sonic line, which is a front of the rear supersonic region. The spacing between the shock and sonic line decreases as the free-stream Mach number increases; however, it cannot vanish because the shock and sonic line cannot have a common point on the airfoil. Therefore, if M_∞ exceeds a certain value, then the shock wave jumps downstream and creates a coalescence of the bow and rear supersonic regions. In the 3D flow over wings, the supersonic regions may coalesce either gradually or abruptly, depending on the wing sweep angle [7].

In this paper, we study the interaction of local supersonic regions on an axisymmetric projectile. Free-stream Mach numbers, at which the coalescence/rupture of the supersonic regions occurs, are determined.

2. FORMULATION OF THE PROBLEM

To study peculiarities of the 3D flow over a projectile, we choose a profile constituted by the

$$\text{circular arc } (x-4)^2 + (y+7.5)^2 = 8.5^2, \quad 0 \leq x \leq 4; \quad (1a)$$

$$\text{horizontal segments } y=1, \quad 4 \leq x \leq 6.4; \quad (1b)$$

$$\text{vertical segment } x=7, \quad 0 \leq y \leq 0.73; \quad (1c)$$

$$\text{a parabolic arc connecting these segments,} \quad (1d)$$

see Figure-1. In what follows, the Cartesian coordinates (x, y, z) are dimensional and given in centimeters. A rotation of the profile (1) about the x -axis creates the 2D surface of a projectile model at zero incidences to the free stream, which is parallel to the x -axis. Then a rotation of the projectile about the z -axis sets it at an angle of attack $\alpha=6$ deg.

For CPU time savings, we assume the flow to be symmetric about the plane $z=0$. This makes it possible to perform computations only in a domain located at $z>0$.



The outer boundary of the computational domain is created by a rotation of the circular arc $(x+525)^2+y^2=725^2$ about the y -axis, see Figure-2.

Let the free stream be uniform, so that the x - and y -components of the incoming flow velocity are

$$U_\infty = M_\infty a_\infty, V_\infty = 0, W_\infty = 0 \text{ at } x=0.$$

Also on the inflow boundary $x=0$ we prescribe the static pressure $p_\infty=75,000 \text{ N/m}^2$ and static temperature $T_\infty=250 \text{ K}$ which determines the sound speed $a_\infty=317.02 \text{ m/s}$. At the outlet, we impose the pressure p_∞ . The no-slip condition and vanishing heat flux are used on the projectile. The free-slip condition was prescribed on the plane of symmetry $z=0$. Initial data were parameters of the free stream. The air is treated as a perfect gas whose specific heat at constant pressure is 1004.4 J/(kg K) and the ratio of specific heats is 1.4. We adopt the value of 28.96 kg/kmol for the molar mass, and use the Sutherland formula for the molecular dynamic viscosity. The Reynolds number based on the projectile length and $M_\infty=0.945$ is 1.19×10^7 .

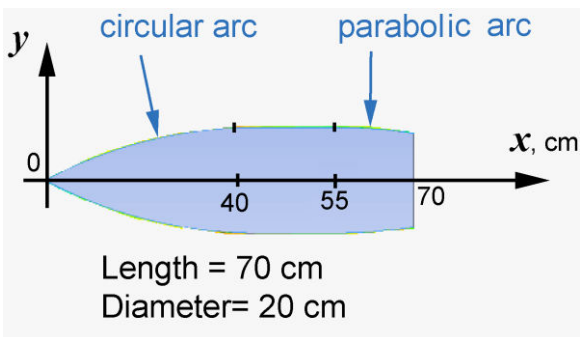


Figure-1. Sketch of the projectile model.

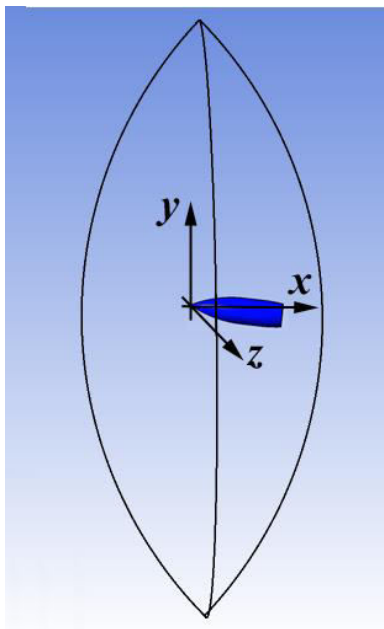


Figure-2. Sketch of the computational domain.

3. A NUMERICAL METHOD

Solutions of the unsteady Reynolds-averaged Navier-Stokes equations were obtained with ANSYS-15 CFX finite-volume solver, which is based on a high-resolution numerical scheme of second-order accuracy in space and time. An implicit backward Euler scheme was employed for the time-accurate computations. In addition, some computations were performed with ANSYS-15 Fluent solver; see Figures 6b and 7 below. We used a Shear Stress Transport $k-\omega$ turbulence model which is known to reasonably predict aerodynamic flows with boundary layer separations [8].

A hybrid unstructured mesh was constituted by about 10^6 hexahedrons in 39 layers on the projectile and by 5×10^6 prisms in the remaining region. The non-dimensional thickness y^+ of the first mesh layer on the plate and wall was less than 1. Apart from the boundary layer region, mesh nodes were clustered in vicinities of the shock waves. Test computations on uniformly refined meshes of approximately 3×10^6 , 6×10^6 , and 12×10^6 cells showed that a discrepancy between shock wave coordinates obtained on the second and third meshes did not exceed 2%. Global time steps of 10^{-5} s and $2 \times 10^{-5} \text{ s}$ yielded undistinguishable solutions. That is why we employed meshes of 6×10^6 cells and the time step of $2 \times 10^{-5} \text{ s}$ for the study of 2D transonic flow at various free-stream velocities. The root-mean-square CFL number (over mesh cells) was about 4.

The solver was verified by computation of a few commonly used 3D test cases, in particular, transonic flow over an ONERA M6 wing [9].

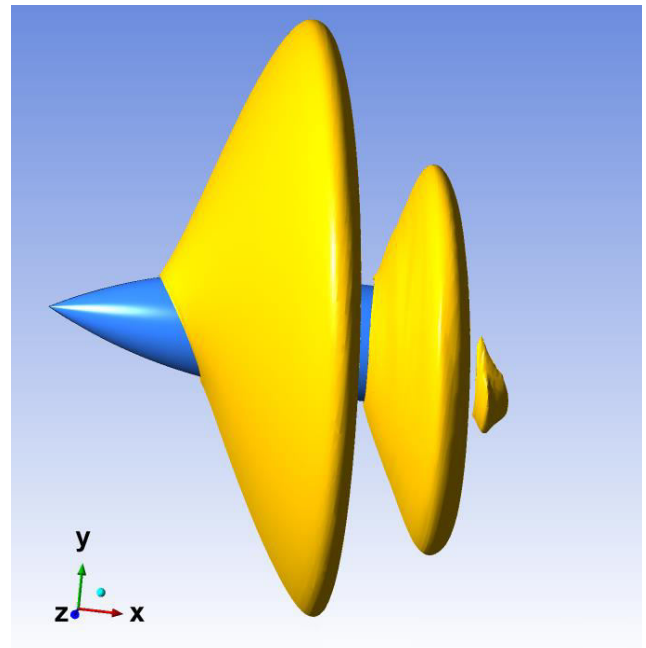


Figure-3. Isosurface $M(x,y,z)=1$ in turbulent flow at $M_\infty=0.9325$.



4. RESULTS AND DISCUSSIONS

First, we performed the numerical simulation at $M_\infty=0.9325$. Computations showed a convergence of the mean parameters of turbulent flow to a steady state in less than 0.15 s of physical time. The obtained flow field exhibits two separate supersonic regions on the projectile. Each region is terminated by a shock wave, behind which the flow velocity is subsonic, see Figure-3.

When M_∞ increases, the leading supersonic region grows and expands (see Figure-4). At $M_\infty=0.9402$ it gets in touch with the rear supersonic region on the lower surface of the projectile. This is in contrast to a typical behavior of transonic flow over flat-sided symmetric airfoils where the local supersonic regions get into coalescence first on the upper surface of the airfoil and after that, at larger values of M_∞ , on the lower one.

Figure-6 shows static pressure distributions over the projectile in the plane of symmetry at $M_\infty=0.944$. As seen, there are only negligible distinctions between flow fields calculated with ANSYS CFX and Fluent solvers. Figure-7 exhibits the static pressure on the upper and lower surfaces of the projectile in the plane of symmetry.

Figure-8 presents the coefficient $m_z=2M_{pitch}/(\rho_\infty U_\infty^2 S \times 0.7[\text{m}])$ of the pitching moment about the origin as a function of M_∞ , where ρ_∞ is the free-stream density and $S=0.56297 \text{ m}^2$ is the square of the half a projectile in planform. In the band $M_\infty < 0.9384$ (see part (a) of the plot) where the flow exhibits two separate supersonic regions, the slope of the plot is small. In the band $0.939 < M_\infty < 0.9445$ (part (b) of the plot) the local supersonic regions are merged on the lower surface of the projectile. In this band the moment coefficient rises and then decreases, exhibiting a local maximum. Finally, at $M_\infty > 0.9445$ (see part (c)) the local supersonic regions merge on the upper surface as well, whereas the pitching moment coefficient demonstrates a pronounced local minimum, after which it abruptly rises. In contrast to 2D flow over airfoils, the coalescence of supersonic regions does not cause jumps of $m_z(M_\infty)$. This is accounted for by an essential correlation between flow parameters on the upper and lower surfaces of the projectile due to their interaction via the circumferential direction.

Inversely, if M_∞ decreases step-by-step from $M_\infty=0.965$ to $M_\infty=0.9325$ then the supersonic region shown in Figure-9, first, shrinks, then ruptures on the upper surface of the projectile and after that does so on the lower one. Further decrease of M_∞ causes a gradual displacement of the leading supersonic region upstream and an increase of the distance between two supersonic regions.

We notice that a similar evolution of the flow field develops with increasing angle of attack α from 0 to 8 deg at a fixed M_∞ . This is in agreement with results obtained in the papers mentioned in Introduction.

5. CONCLUSIONS

The numerical simulation of 3D transonic flow over the projectile (1) showed two major distinctions from transonic flow over flat-sided airfoils. A first distinction is that, with increasing free-stream Mach number, the local supersonic regions get in contact and coalescence, first, on

the lower side of the projectile and then on the upper side. A second distinction is that the coalescence (or a rupture of the supersonic regions with decreasing M_∞) does not produce noticeable jumps of the aerodynamic coefficients. Maxima and minima of the pitching moment coefficient $m_z(M_\infty)$ do not coincide with free-stream Mach numbers at which the local supersonic regions get into coalescence on the projectile.

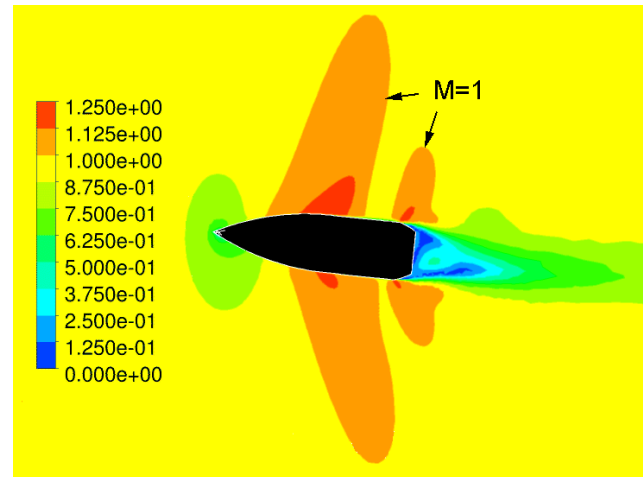


Figure-4. Mach number contours in the plane of symmetry $z=0$ at $M_\infty=0.938$.

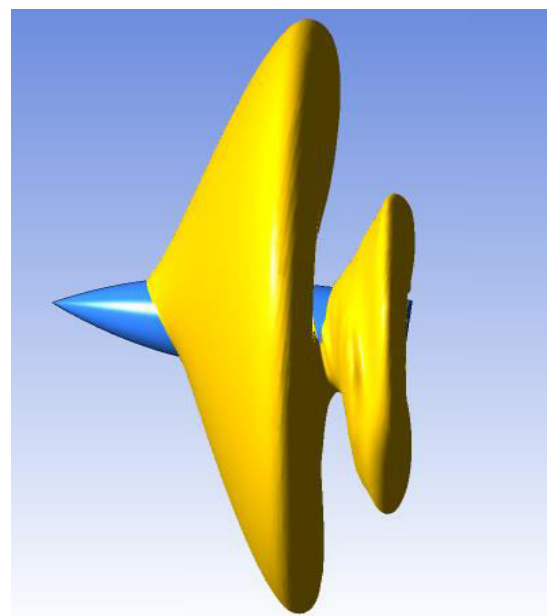


Figure-5. Isosurface $M(x,y,z)=1$ in the flow at $M_\infty=0.941$.

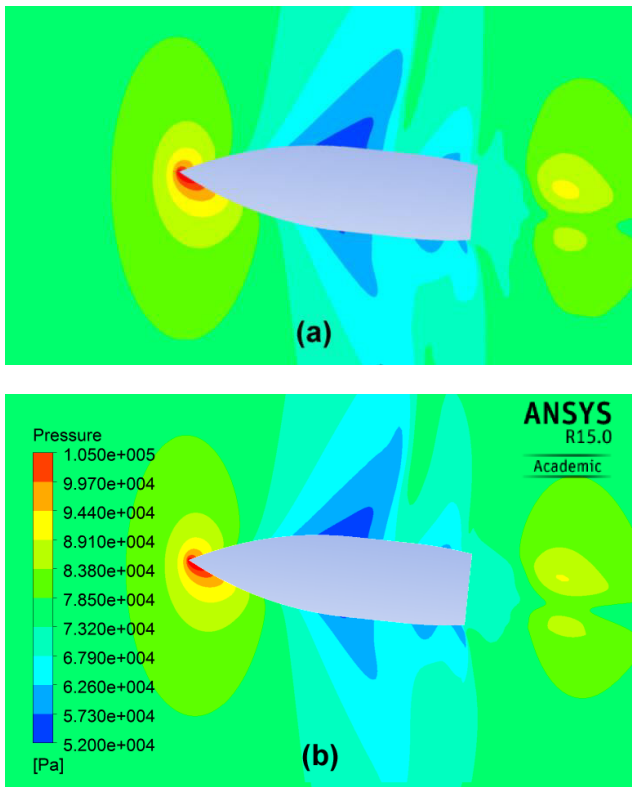


Figure-6. Contours of the static pressure in the plane of symmetry $z=0$ at $M_\infty=0.944$. Computations with: (a) CFX, (b) Fluent.

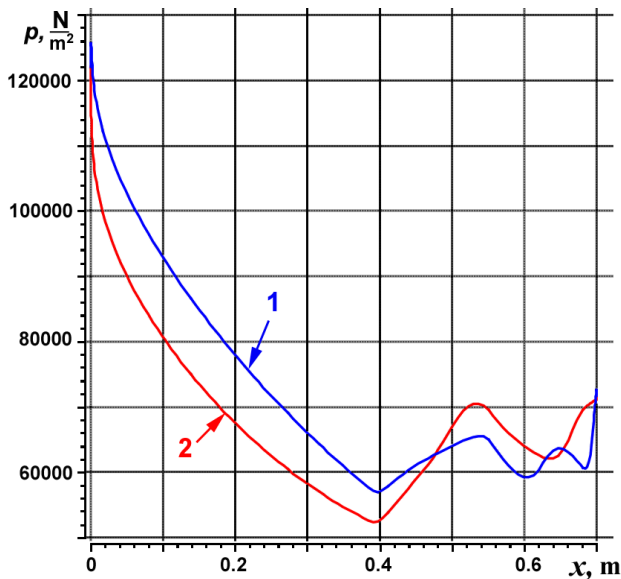


Figure-7. Static pressure distribution on the lower (curve 1) and upper (curve 2) surfaces of the projectile in the plane of symmetry $z=0$ at $M_\infty=0.944$. Computations with ANSYS -15 Fluent.

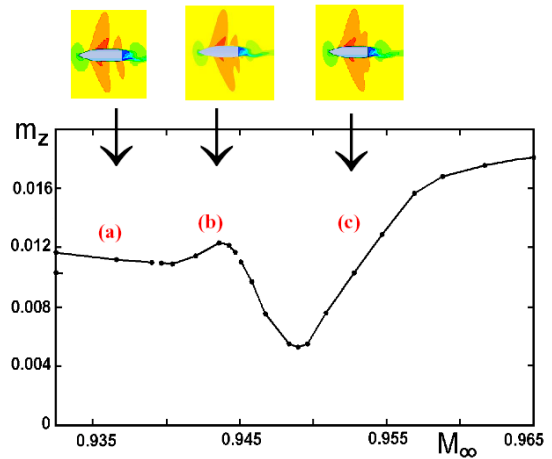


Figure-8. The pitching moment coefficient m_z versus M_∞ .

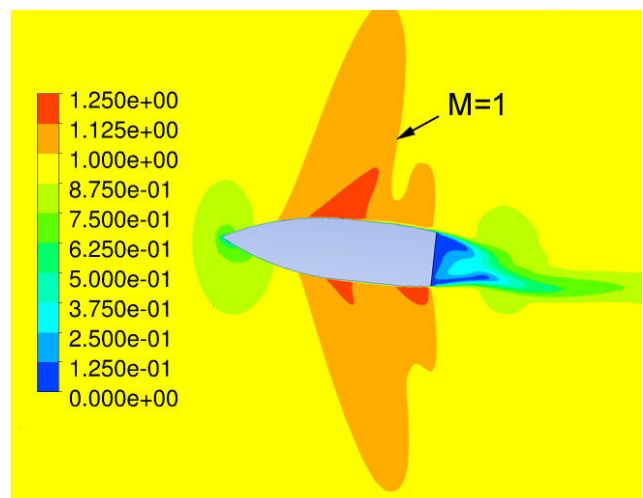


Figure-9. Mach number contours in the plane of symmetry $z=0$ at $M_\infty=0.948$.

ACKNOWLEDGEMENTS

This research was performed using computational resources provided by the Computational Center of St. Petersburg State University (<http://cc.spbu.ru>).

REFERENCES

- [1] Sahu J., Nietubicz C. J. 1994. Three-dimensional flow calculations for a projectile with standard and dome basis. J. of Spacecraft and Rockets. 31(1): 106-113.
- [2] Budge A. M. 1998. Aerodynamic fuze characteristics for trajectory control. Master's thesis, Massachusetts Inst. of Technology, Department of Aeronautics & Astro-nautics, USA.
- [3] Lun S. W. 2011. Aerodynamic validation of emerging projectile configurations. PhD thesis, Naval Postgraduate School, Monterey, California.



- [4] Jameson A. 1991. Airfoils admitting non-unique solutions of the Euler equations. AIAA Paper 91-1625, pp. 1-13.
- [5] Kuzmin A. 2012. Non-unique transonic flows over airfoils. Computers and Fluids, 63: 1-8.
- [6] Kuzmin A., Ryabinin A. 2014. Transonic airfoils admitting anomalous behavior of lift coefficient. The Aeronautical J. 118 (1202): 425-433.
- [7] Kuzmin A. 2015. Sensitivity analysis of transonic flow over J-78 wings. Int. J. Aerospace Engineering. Hindawi. Vol. 2015. Article ID 579343, pp. 1-6.
- [8] Menter F. R. 2009. Review of the Shear-Stress Transport turbulence model experience from an industrial perspective. Int. J. Comp. Fluid Dynamics. 23: 305-316.
- [9] Kuzmin A. 2014. On the lambda-shock formation on ONERA M6 wing. Int. J. Applied Engineering Research. 9(20): 7029-7038.